

Comparison of transient thermography methods for defect detecting in electronic components and modules

Anna Andonova

Dept. of Microelectronics
Technical University of Sofia
Sofia, Bulgaria
ava@ecad.tu-sofia.bg

Abstract—The article examines different methods of transient thermography applied to analyze the faults and detection of hidden defects in electronic components and modules. A brief analysis of the methods and recommendations for their application is presented. A systematic approach to designing a transient thermographic measurement system for the detection and analysis of faults and hidden defects in electronic components and modules is developed. Some experimental results are shown.

Keywords—*fault diagnostic; transient thermography; electronic components and modules; quality;*

I. INTRODUCTION

The heat control is a useful technique for non-destructive detection of hidden defects and analysis of faults in electronic components and modules. Methods of active thermography successfully are invoked as a powerful tool for diagnostics and preventive control in the manufacture of electronic components and modules in the fight to reduce the cost of quality.

Infra-red thermography is called active (transient) or dynamic, where the detection of internal defects depends significantly on the time of detection or the time of observation (observation time). Active thermography offers a fast, reliable and clear means of retrieving information about the structure of the object and its defects. Analysis of the amendment of the thermal gradient and the contrast, the phase and amplitude over time is also of interest for the development of thermographic measuring algorithms for increase the signal/noise ratio [1, 4, 10, 12].

The heat source is periodically activated in the dynamic infrared thermography, and the surface of the tested electronic component/module is monitored by infrared (IR) camera. With computer processing of the raw thermograms can achieve the modulation of the surface temperature of the order of a hundred mK. An advantage of the transient thermography is the effective spatial resolution that can be significantly improved due to the suppression of the lateral diffusion of the heat.

Serious limitations are related to the wavelength of the IR camera (with a range $1,5 \div 3 \mu\text{m}$, $3 \div 5 \mu\text{m}$ and $7,5 \div 12 \mu\text{m}$), such as at wavelengths $3 \div 5 \mu\text{m}$ spatial resolution is $5 \mu\text{m}$. Nevertheless dynamic thermography allows detection of

defects in electrical components and modules, when their power exceeds $10 \mu\text{W}$. Dynamic quantitative thermography can be applied in two varieties:

- For faults and defects related to locally generate heat – breakdowns, metallization shorting, leakages;
- For faults and defects that are not associated with locally heat generation - breaks, cracks, missing adhesion between the layers.

Heat sources are activated by means of variable electrically signals for powering the test electronic products in the first variant. The second group uses an external heat source (halogen lamp, laser, flash, infrared light, acoustic transducer).

Present are developing several forms of dynamic thermography: pulse, pulse-phase, frequency-modulated, phase-sensitive or synchronized (more popular as lockin) and heating step. Sometimes it can be used static infrared thermography for this purpose. In the latter case, however, there are two major limitations - limitations on the spatial resolution due to the wavelength of the technique and shown strong emissivity (IR-emissivity) contrast (ε -contrast), which obscures the thermal contrast. In general ε -contrast can be compensated, but it requires time, a more complex procedure and is not always successful.

II. FAULTS AND HIDDEN DEFECTS DETECTION BY TRANSIENT THERMOGRAPHY

Fig 1 depicts the basic elements of an IR transient thermal imaging system: 1- a thermal excitation source; 2 - a target (electronic component or module); 3 - a radiometer (IR camera); 4 - a signal control, image analysis and result display system (PC). The signal degradation is omnipresent at all stages. If a thermal gradient between the scene and the electronic component/module exist, the target can be inspected using the passive approach. However, when the target is in equilibrium with the rest of the scene, it is possible to create a thermal contrast on the surface using a thermal excitation source (source of electrical or optical signal), this is known as the active approach in IR thermography. No matter what the active or passive approach is used, IR signatures are weak when compared with other forms of radiation. The IR radiation

measured by the radiometer results from the contribution of three different sources: the thermal energy emitted from the object; the energy reflected from the background; and the energy transferred through the material. Additionally, the atmosphere attenuates the oncoming thermal signatures. A radiometer (IR camera) 4 captures the (weak and noisy) thermal signatures coming from the target. Here again, every element of the IR camera contributes to further degrade the signal, i.e. optical, electronic and electromagnetic noise. As a result, a data processing step 5 is generally required. Various IR image processing techniques are used depending on the nature of the transient thermography. These techniques are intended to reduce noise at pre and post processing stages, to enhance image contrast and to retrieve useful information from the images. Finally, the resulting processed data must provide qualitative or quantitative outputs allowing the conditions of the target to be assess.

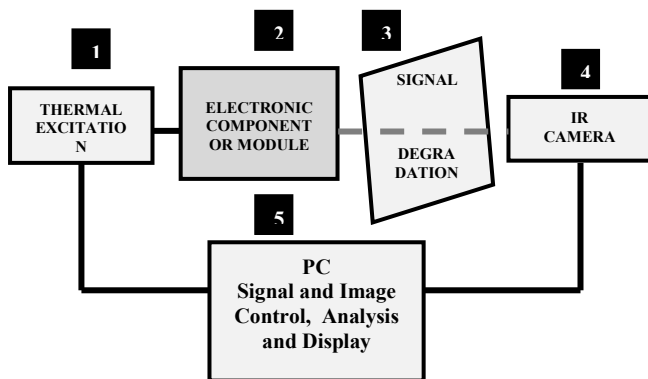


Fig. 1. The IR transient thermal imaging system

A. Pulsed Thermography (PT)

In a PT experiment, data are obtained by heating the sample with a pulse stimulus and observing the temperature decay T(t). The temperature of the specimen changes rapidly after the initial thermal pulse because the thermal front propagates, by diffusion, under the surface and also because of radiation and convection losses. The presence of a hidden defect reduces the diffusion rate so that when observing the surface temperature, defects appear as areas of different temperatures with respect to surrounding sound areas once the thermal front has reached them. Consequently, deeper defects will be observed later and with a reduced contrast.

The observation time t is function (in a first approximation) of the squared of the depth z and the loss of thermal contrast C is proportional to the cube of the depth

$$t \approx \frac{z^2}{\alpha} \quad C \approx \frac{1}{z^3} \quad (1)$$

where a is the thermal diffusivity of the material.

There are many processing techniques such as: thermal contrast, differential absolute contrast, principal component analysis, thermographic signal reconstruction, statistical analysis, fit the thermographic data to an experimental curve [2, 3, 4].

Two limitations of the IRT are important: observable defects will generally be shallow and the thermal contrasts will be weak. The radius of the smallest detectable defect should be at least one to two times larger than its depth under the surface. This rule is valid for homogeneous isotropic material. In case of anisotropy it is more constrained.

For the shallowest defect, pulsed thermography produces the best signal-to-noise ratio.

Result from experimentam application of PT is shown on Fig. 2.

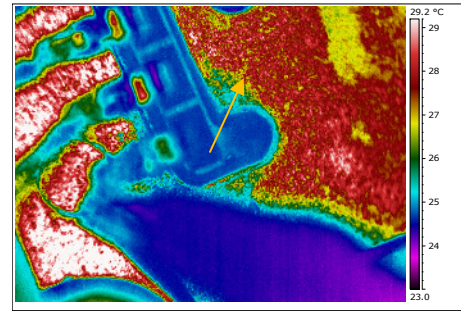


Fig. 2. Hidden defect under layer of plastic detected by PT

B. LockIn Thermography (LIT)

The different points of view between electronic components/module testing and non-destructive testing leads to different technical requirements to the lockin thermography. The spatial resolution should be as good as possible in electronic product, hence here the lock-in frequency should be able to be chosen as large as possible for effectively suppressing lateral heat diffusion [1].

In electronic specimen the synchronization of the camera frames to the lock-in trigger is trivial, so the results are displayed as amplitude- and phase images, as well as the display of a certain phase component (0° or -90° signal).

In electronic specimen the bias applied is usually modulated rectangular, since electronic components are usually nonlinear devices. The demands on the detection sensitivity are certainly stronger for electronic components and their dissipated power is limited.

Lock-in thermography works on the principle that the heat sources are periodically intensity-modulated at a certain lock-in frequency. So only the local temperature modulation is evaluated according to the lock-in principle and averaged over many lock-in periods.

Since in LT two-channel lock-in correlation is used, the phase image can be displayed where the emissivity contrast is inherently compensated.

Mathematically this correlation procedure is a discrete Fourier transformation of the temperature signal, thus the 0° signal represents the real part and the -90° signal the inverse of the imaginary part of the Fourier transform of the basic harmonic of the temperature.

A typical result of a lockin investigation of a faulty Hall sensors device in coloured picture is shown in Fig. 3. The position of the actual fault is marked by an arrow.

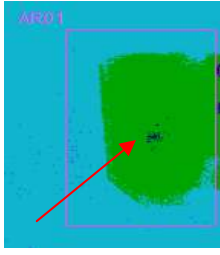


Fig. 3. Hidden defects in packaged Hall sensors detected by LT

C. Pulsed Phase Thermography (PPT)

PPT has been introduced as a technique that combines together the advantages of Modulated Thermography (MT) and Pulsed Thermography (PT). Several techniques have been considered for quantitative PPT, for instance: statistical methods [5], Neural Networks [6], wavelets [7], Fourier analysis[8]. PPT uses the experimental procedure from PT and the data analysis technique from MT. It is based on the Fourier Transform (FT) of sampled thermal decay $T(t)$. Consider the 1D analytical solution of the Fourier equation for the cooling stage of a plate of thickness L and thermal diffusivity α heated with a square pulse of power density Q and duration t_h (in this case t_h is short enough to consider the stimulus as an instantaneous pulse):

$$T(t) = \frac{Q}{h} \sum_{n=1}^{\infty} \frac{2Bi}{Bi(Bi+1) + \mu_n^2} e^{-\mu_n^2 F_0} (e^{\mu_n^2 F_{oh}} - 1) \quad (2)$$

where h is the surface heat exchange coefficient, Bi the Biot Number, μ_n the positive roots of the equation $\mu \tan(\mu) = Bi$, F_0 and F_{oh} respectively the Fourier number for t and t_h . The analytical expression of the Fourier transform of (1) is

$$\theta(f) = \frac{Q}{h} \sum_{n=1}^{\infty} \frac{2Bi}{Bi(Bi+1) + \mu_n^2} \left(1 - e^{-\mu_n^2 F_{oh}}\right) \frac{e^{-j2\pi f t_h}}{(\mu_n^2 \alpha) / L^2 + j2\pi f} \quad (3)$$

A typical output of PPT algorithm is an image with each pixel representing the magnitude and phase at a fixed frequency as shown in Fig.4.

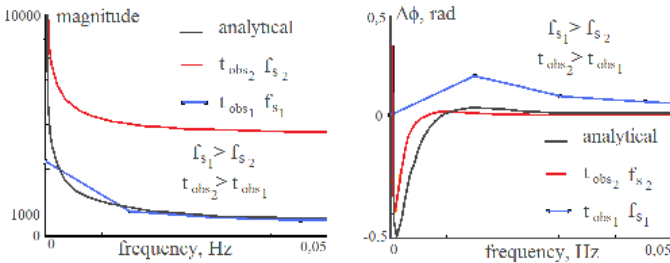


Fig. 4. Amplitude (magnitude) and phase difference of the simulated thermal profile

Hence, defect visibility is a function of the phase difference, $\Delta\phi$, between a reference point and a defect. Therefore, considering the phase difference as the informative parameter, more specifically of interest is the maximum absolute value that gives the best signal to noise ratio.

Result from PTT measurements is shown on Fig. 5

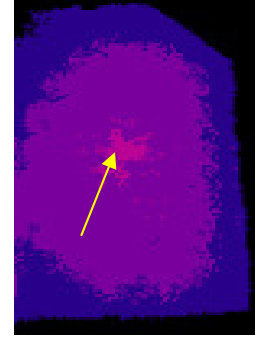


Fig. 5. Hidden defects in packaged Hall sensors detected by PTT

D. Frequency Modulated Thermography (FMT)

The wavelength in FMT is not fixed but varies as a function of frequency m during the experiment, leading to variation in the depth resolution for detection of defects at different depths. Frequency modulated thermal wave imaging (FMTWI) is a superposition of multiple LIT experiments [12]. Objective comparison of pulsed, LIT, and FMTWI is not easy. A comparison based on computed signal-to-noise ratio (SNR) under matched energy condition has been summarized by [12].

Presently in FMT, a linear up-chirp is used. The phase f of such a signal is related to time t as [12]

$$\phi(t) = 2\pi \left(f_i + \frac{kt}{2} \right) t + \phi_i \quad (4)$$

where f_i is the initial frequency of the chirp, k is the frequency slope and ϕ_i is the initial phase, i.e. phase at time $t = 0$. The terminal phase and the initial phase of the chirp should differ only by integral multiples of 2π . During the Fourier transformation of the signal, high frequency components would be generated due to the presence of discontinuities at the repetition boundaries. Hence the initial phase ($\phi_{|t=0}$) and the final phase ($\phi_{|t=\tau}$) of the chirp should be related to each other by

$$(\phi_{|t=\tau}) = (\phi_{|t=0}) + 2\pi \quad (5)$$

where τ is the duration of the chirp and n is the number of oscillation the signal completes in τ . This relates the chirp bandwidth, its duration and the number of complete oscillations as

$$\tau = \frac{2n}{f_i + f_f} \quad (6)$$

where f_f is the final frequency at $t = \tau$.

High peak power heat source requirement in pulsed thermography, and limited depth resolution of lock-in thermography due to fixed modulating frequency of sources, are overcome by the FMT.

Application of SPT is shown on Fig.6.

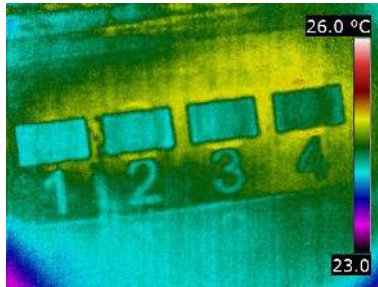


Fig. 6. Amplitude (magnitude) and phase difference of the simulated thermal profile.

E. Step heating thermography (SPT)

Step heating uses a larger pulse (from several seconds to a few minutes). The temperature decay is of interest; in this case, the increase of surface temperature is monitored during the application of a step heating pulse. Variations of surface temperature with time are related to specimen features as in PT. [9, 10]. This technique finds applications such as for coating thickness evaluation (including multi-layered) and for determination of coating-substrate bond integrity. The empirical relationship [9] providing the coating thickness L is

$$t_c = 0,36L^2/\alpha \tag{7}$$

where t_c is the thermal transit time and α is the thermal diffusivity. In such experiments, the electronic component/module is heated and the temperature is plotted versus the square root of time, Fig. 7. The thermal transit time is observed when the curve begins to depart from the semi-infinite case (which is a straight line in such plots). For the heating which is constant during the measurement, for instance can be used a laser.

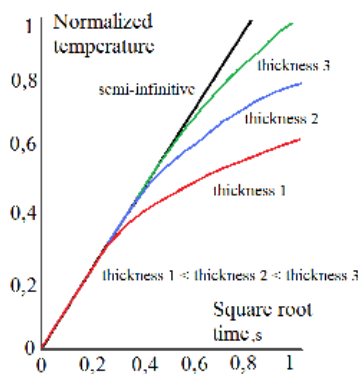


Fig. 7. Temporal evolution of normalized temperature layers of different thickness for step heating pulse

The method is suitable for the detection and characterization of deeply located defects in metal, ceramic and polymer layers of electronic components and modules.

Since the duration of the heating pulse is longer, it can control the temperature of heating, in order to avoid destruction of the specimens.

III. SYSTEMATIC APPROACH TO FAILURE ANALYSIS THROUGH ACTIVE THERMOGRAPHY

Flow diagram for the application of transient thermography in the detection of defects and analysis of faults of electronic components and modules is shown on Fig. 8.

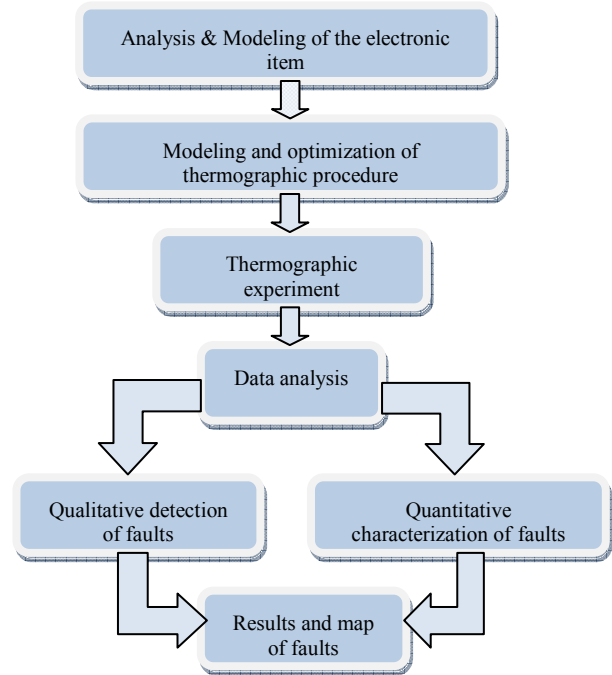


Fig. 8. Technology of the transient thermography

Thermophysical characteristics of the electronic item are: basic – thermal conductivity (K , $W \cdot m^{-1} \cdot K^{-1}$); specific heat capacity (c , $J/(kg \cdot K)$); density (ρ , kg/m^3) and dynamic –thermal diffusivity or diffusion length (α , m^2/s); thermal effusivity or thermal inertia (e , $W \cdot m^{-2} \cdot s^{1/2} \cdot K^{-1} \cdot m^{-2}$ or $J \cdot m^{-2} \cdot K^{-1} \cdot s^{1/2}$). Thermo physical characteristics of the electronic item, the depth and size of defects in them determine the amplitude of the temperature signal over the defect, the type of methods used and the time of its discovery. The marginal parameters of the detected defects are determined by the level of noise. When the experiment is properly constructed should be predominant noise of the controlled target.

Requirements for equipment of the transient thermography (frame rate, power and duration of heating, type of thermographic method) are determined by the properties of the object under control.

The real object is replaced with a simple theoretical models in numerical modeling (using FEM, CFD). Analytical solutions or numerical modeling are used and the dynamics of

temperature is analyzed for the models depending on the dimension (1 - D, 2 - D or 3D-model) [13].

By means of modeling of particular transient thermography procedure may be carried out the optimization of the experiment, taking into account the possible practical limitations. After optimization of the experiment a temperature function $T(i, j, \tau)$ that is determined for each point of the object under control was prepared.

The analysis of experimental data is carried out using specialized software programs. The aim is to find fault with given statistical properties such as the probability of correct detection and probability of false alarm. If a defect is discovered it is possible to estimate its parameters by solving the inverse problem of thermal control. The control procedure ends with the drawing a carats of the defects - binary images in which, for example 1 is attached to the pixels relating to defective areas and 0 - to the pixels from the defect-free areas.

IV. CONCLUSIONS

SPT is preferred for analysis of the failure based of migration. SPT can early to detect this kind of fault and limit heating during diagnostic. The discovery of shallow cracks, delamination, short circuit, bad hermetization can be successfully evaluated with PT. Demand for deep hidden defects should be done with LIT or FMT. The choice of one or the other method will depend on the design and technology features of the electronic device, the signal/noise ratio and the observation time.

Using the methods of transient thermography provides new opportunities for analysis of failures and non-destructive diagnostics of electronic components and modules on the way to improve the quality of their production.

ACKNOWLEDGMENT

The study was made possible through the financial support of NSF project DFNI-I01 "Information Measurement System for Thermographic Evaluation of Potential Failures and Life

Prediction of High Reliability Energy Transformation Elements".

REFERENCES

- [1] O. Breitenstein, "Lock-in IR Thermography for Functional Testing of Electronic Devices", 7th Int. Conf. on Quantitative Infrared Thermography (QIRT 2004), Rhode-St.-Genese, Belgium, 6.7.2004, Proceedings pp. B.3.1-6
- [2] C. Ibarra-Castanedo, D. Gonzalez, Galmiche F., A. Bendada, X. Maldague, "Recent Research Developments in Applied Physics On signal transforms applied to pulsed thermography" Recent Research Developments in Applied Physics, vol.9, pp. 101-127, 2006.
- [3] C. Ibarra-Castanedo, M. Genest, P. Servais, X. Maldague, A. Bendada, "Qualitative and quantitative assessment of aerospace structures by pulsed thermography", *NDT & E*, vol. 22(2-3), pp.199-215, June-September 2007.
- [4] V. Vavilov, *Infrared thermography and thermal control*, Moscow, Spectr, 2009 (in Russian)
- [5] <http://www.cs.odu.edu/~mln/ltrs-pdfs/NASA-99-spie-sm.pdf>
- [6] M. Vallerand, X. Maldague, "Defect Characterization in Pulsed Thermography: A Statistical Method Compared with Kohonen and Perceptron Neural Networks," *NDT&E Int.*, **33**(5), pp. 307-315, 2000.
- [7] X. Maldague, Y. Lergouët, J. Couturier, "A Study of Defect Depth Using Neural Networks in Pulsed Phase Thermography: Modeling, Noise, Experiments," *Rev. Gén. Therm.*, **37**:704-717, 1998.
- [8] F. Galmiche, X. Maldague, "Depth defect retrieval using the wavelet pulsed phased thermography", <http://qirt.gel.ulaval.ca/archives/qirt2000/papers/036.pdf>
- [9] Xavier Maldague, "Applications of infrared thermography in nondestructive evaluation", http://w3.gel.ulaval.ca/~maldagx/r_1123.pdf
- [10] http://www.visioimage.com/en/products_ir_ndt_thermography_tutorial.htm
- [11] A. Badghaish, D. Fleming, "Non-destructive Inspection of Composites Using Step Heating Thermography", *Journal of Composite Materials* vol.42, pp. 1337-1357, July 2008
- [12] K. Chatterjee, S. Tulia, S. G. Pickering, and D. P. Almond, "An objective comparison of pulsed, lock-in, and frequency modulated thermalwave imaging", *AIP Conference Proceedings*, 1430. pp. 1812-1815, 17-22 July 2011.
- [13] D. Peng, R. Jones, "Modelling of the lock-in thermography process through finite element method for estimating the rail squat defects", *Engineering Failure Analysis* vol. 28, pp. 275-288, 2013.